Available online at www.sciencedirect.com
SCIENCE DIRECT®
ELSEVIER
Optics and Lasers in Engineering 44 (2006) 159–169
OPTICS and LASERS in ENGINEERING

Investigation of the properties of a sharp-focusing schlieren system by means of Fourier analysis

Axel Hanenkamp, Wolfgang Merzkirch*

Lehrstuhl für Strömungslehre, Universität Essen, D-45117 Essen, Germany

Available online 31 May 2005

Abstract

The sharp-focusing schlieren system is analysed by means of a Fourier approach. The signal received in the imaging plane is governed by the phase distribution in a particular object plane normal to the optical axis, while the contributions from other planes in the object that are out-of-focus can be considered as noise. A numerical simulation performed for a specific test object shows that the best spatial resolution is obtained with a system of five channels and that further increase of the number of channels does not improve the signal quality.

Keywords: Visualization; Schlieren; Fourier optics

1. Introduction

The schlieren method makes use of the refractive deflection of light in an optical phase object, e.g. a flow with varying fluid density, for generating a visible signal that provides information on certain properties of the object. In the case of a fluid flow the signal is a measure of the density gradient; see, e.g., Settles [1]. Like in any "line-of-sight" method, the information on the density distribution in the flow is integrated along the light path through the object (in the following analysis the z-direction). It follows that the dependence of the density on the z-coordinate cannot be determined with a "conventional" schlieren system in which one light beam

*Corresponding author. Tel.: +49 234 793350; fax: +49 234 793350.
E-mail address: wolfgang.merzkirch@uni-essen.de (W. Merzkirch).

0143-8166/$ - see front matter
doi:10.1016/j.optlaseng.2005.04.003

traverses the test object. In order to overcome this problem and provide a three-dimensional (3D) resolution of the object's properties, a modification of the schlieren system was proposed by Kantrowitz and Trimpi [2]. They used a multiple of light sources with a light beam or "channel" originating from each source and traversing the 3D object with different angular directions. The image plane where all channels overlap is focused onto a particular plane in the object, normal to the z-direction, and the information from the overlapping signals is a measure of the desired quantity, in our example the fluid density gradient, in the focused object plane. This proposed method that the authors had called a "sharp-focusing schlieren system", was later improved and further developed for practical use by Weinstein [3]. Collicott and Salyer [4] pointed out that this name is misleading and that "multisource system" would be more adequate.

We present here the results of a Fourier analysis of the sharp-focusing schlieren system that serve for exploring the potentials of this method for providing a spatial resolution of the test object. The sharp-focusing system can be regarded as a multi-channel system, i.e., a superposition of a finite number of conventional (single channel) schlieren systems. Therefore, we first give a summary of the Fourier analysis of the conventional system as it was reported in the literature (see below). Details of the derivations for the multi-channel system can be found in the thesis of Hanenkamp [5]. Although this thesis is written in German, the derivations of the respective formulae are self-explanatory and can be followed easily. A Fourier description of the multi-channel system was also presented by Collicott and Salyer [4]. The aim of their analysis was to explore the influence of phase perturbations outside the test field onto the signal quality and the possible reduction of these disturbances by applying the multi-channel system.

Each channel of the multi-channel system "views" the object in a different direction in space and collects different two-dimensional (2D) information on the object's spatial (3D) properties. The idea is that the 3D object can be reconstructed from this multitude of 2D information. Another and perhaps more effective approach for resolving the information from an extended, three-dimensional object is optical tomography. Therefore, we present a short comparison of the multi-channel system and optical tomography in the discussion at the end of the paper. The present Fourier analysis is not accompanied by experiments. For experimental results and details we refer to the work of Weinstein [3] and applications of the "sharp-focusing schlieren system" reported, e.g., by Taghavi and Raman [6] and Garg and Settles [7].

2. Fourier analysis

2.1. Conventional schlieren system

Fourier analyses of the conventional schlieren system were presented, e.g., by Wolter [8] and Lopez [9]. In following these approaches we regard here a set-up with the point source located in the focus of the first lens, a phase object placed in the

diverging light beam in front of the first lens, the knife edge (filter) in the rear focal point of the first lens, and a second lens forming an image of the object (Fig. 1). The optical axis is the z-axis; the functions describing the optical elements at selected positions z_i (lenses, filter, etc.) are taken as one-dimensional such that they depend only on x. The object placed at position z_2 is described by a function $t_2(x)$. The first lens at z_3 produces a virtual image of $t_2(x)$ at z'_2 with magnification m'. The knife edge (filter) at z_4 is in the conjugate plane of z_1, the position of the light source. The second lens at z_5 maps the virtual image t'_2 onto the (final) image plane z_7. Since, in a later step, we consider a possible extension of the object in the z-direction, we make use of an (arbitrary) plane of observation at z_6 so that the application of the lens law, linking z'_2 with z_7, as an additional constraint is avoided.

The signal received in the plane of observation is the light amplitude or intensity. For a two-lens system like the one shown in Fig. 1 the signal transmitted to the position z_6 can be analysed with the functional tools formulated, for e.g., by Gaskill [10]. After a series of steps in the calculation (for details see [5]) one arrives for the light intensity at position z_6 with

$$u_6(x) = A\left(\frac{j}{b}\right)\left(\frac{z_{45}z_{13}z'_{24}}{z_{56}z_{12}z'_{25}}\right)^2 \exp(\mathrm{j}kz_{23})B_{36}B_{\mathrm{L}1}B_{\mathrm{L}2}q\left(x; a_{56} - \frac{a_{56}^2}{b}\right) \times t''_2(x)^*\left\{\left(\frac{-z_{45}m'}{\lambda z_{56}z'_{24}}\right)^2 P_4\left(\frac{-z_{45}m'x}{\lambda z_{56}z'_{24}}\right)^* Q(x;\hat{c})\right\}. \quad (1)$$

In this equation the z_{ij} are distances between positions z_i and z_j, $B_{\mathrm{L}11}$, $B_{\mathrm{L}22}$ describe the light attenuation in the two lenses, $a_{ij} = 1/\lambda \cdot z_{ij}$ with $\lambda =$ light wave length, b and $\hat{c}$ are combinations of a_{ij}'s, A describes the initial light amplitude; $\exp(\mathrm{j}kz_{23})$ with $k =$ wave number is a phase term describing the wave propagation between z_2 and z_3; $B_{36} = \exp(\mathrm{j}kz_{36})/\mathrm{j}\lambda z_{36}$; $q(x, 1/\lambda z'_{24})$ characterises the dependence of phase on the transverse direction x. The dependence on light wave length λ is weak; for a non-coherent source, an average value of λ should be inserted.The second part of the right side includes two convolutions: The object function $t''2(x)$ (''indicates the

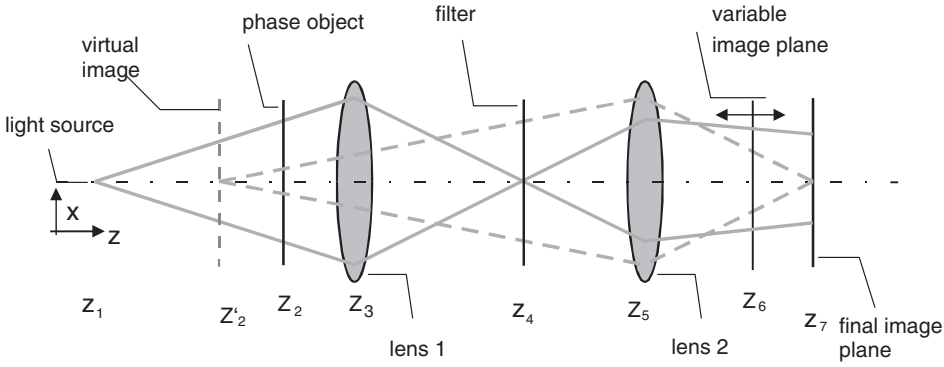

Fig. 1. Optical system with two lenses including a filter at the position of the light source image.

magnification due to the imaging by two lenses) is convolved with the convolution of the filter function P_4 and the function Q that describes the deviation from the final image plane.

According to Eq. (1) the light amplitude at position z_6 as the signal is a double Fourier transform of the object function. If the signal is generated in the exact image plane z_7, Q approaches zero, $Q \to 0$. From Eq. (1), one derives that the impulse response of the system depicted in Fig. 1 is given by

$$h_{26}(x) = \left(\frac{-z_{45}m'}{\lambda z_{56}z'_{24}}\right)^2 P_4\left(\frac{-z_{45}m'x}{\lambda z_{56}z'_{24}}\right)^* Q(x;\hat{c}). \tag{2}$$

The impulse response describes all modulations of light amplitude and phase in the system. The Fourier spectrum of the object is displayed at z_4, the position of the schlieren filter. The knife edge of a conventional schlieren system is a filter that is cutting off a certain part of the spectrum. With the respective filter function P4 one performs a differentiation of the object function by frequency filtering in the frequency domain [8,9]. From this it follows that the image intensity in the recording plane, as the schlieren signal, is proportional to the derivative of the object function. Proper filtering of the spectrum requires the light source image at z_4 to be as small as possible, which is realised by using a point source.

Eq. (1) applies to an infinitesimally thin, one-dimensional object extending in the x-direction, $t_2(x)$, at position z_2. If the object has a finite volume, in the z-direction ranging from ζ_1 to ζ_2 (the y-coordinate is not considered here), then the information on the object is integrated along z in the signal formation, and Eq. (1) is modified to become

$$u_6(x) = \int_{\zeta_1}^{\zeta_2} A\left(\frac{j}{b}\right)\left(\frac{z_{45}z_{13}z'_{24}}{z_{56}z_{12}z'_{25}}\right)^2 \exp(\mathrm{j}kz_{23})B_{36}B_{\mathrm{L}1}B_{\mathrm{L}2}q\left(x; a_{56} - \frac{a_{56}^2}{b}\right) \times \left[t''_2(x,z)^*\left(\frac{-z_{45}m'}{\lambda z_{56}z'_{24}}\right)^2 P_4\left(\frac{-z_{45}m'x}{\lambda z_{56}z'_{24}}\right)^* Q(x;\hat{c})\right] \mathrm{d}z. \tag{3}$$

This equation evidences the known problem common to all line-of-sight methods: the loss of information on the dependence of the object's properties in the z-direction.

2.2. Sharp-focusing schlieren system

The sharp-focusing schlieren system is a superposition of a number of conventional schlieren systems with the (point) light sources of these systems arranged at equal distances along the x-axis at position z_1 (Fig. 2). The light beams originating from these sources pass at different angular orientations through the object, located at z_2 and of which an image is formed by the two-lens system in the plane of observation z_6. Each source has its corresponding filter in the filter plane z_4. Only one light source at an off-axis position $x = x_s$ is shown in Fig. 2. A practical system (see, particularly, Weinstein [3]) has a number of point light sources, say

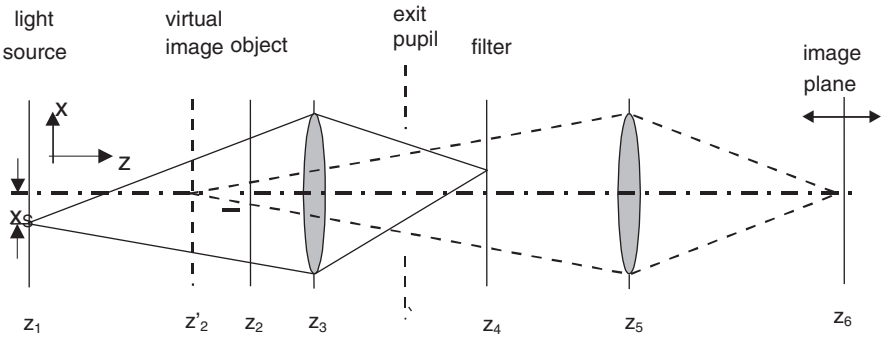

Fig. 2. Optical system as in Fig. 1 but with the light source at an off-axis position.

$2M+1$, with the sources of negative M located below, those with positive M above the optical axis, and the source $M=0$ on the axis; the sources at position z_1 are assumed to be equally spaced along x by the amount x_s. The modelling of the sharp focusing system is performed in two steps: First, the off-axis arrangement with one source as depicted in Fig. 2 is analysed, and then the $K=2M+1$ single systems or "channels" are superimposed to yield the resulting light intensity in the observation plane of this multi-channel system.

The object shown in Fig. 2 is again an infinitesimally thin slice at position z_2. The sharp-focusing system is aimed at providing information on the dependence of the object on the z-direction, which is done by scanning the object in this direction. Therefore, we assume the real object to consist of a number of N parallel (infinitesimally) thin slices, these object "slices" being located at positions z_i with $i=1,\ldots,N$, and characterised by the object functions $t''_{2,i}(x,z_i)$. As outlined in detail in [3] the light intensity distribution in the plane of observation at z_6 is derived as

$$\begin{aligned} u_6(x,z_i) = \sum_{m=-M}^{M}\sum_{i=1}^{N} & A\left(\frac{j}{b_i}\right)\left(\frac{z_{45}z_{13}z'_{24j}}{z_{56}z_{12}z'_{25j}}\right)^2 B_{36,i}B_{L1}B_{L2}\exp(\mathrm{j}kz_{23,i}) \\ & \times q_i\left(x;a_{56}-\frac{a_{56}^2}{b_i}\right)[\exp[\mathrm{j}\pi a_{12}(mx_S)^2] \\ & \times \exp[-\mathrm{j}2\pi a_{12}(mx_S)x] \\ & \times [t''_{2,i,m}(x)^*\left(\frac{-z_{45}m'_i}{\lambda z_{56}z'_{24,i}}\right)^2 P_{4,i}\left(\frac{-z_{45}m'_i x}{\lambda z_{56}z'_{24,i}}\right)^* Q_i(x;\hat{c}_i)]. \end{aligned} \tag{4}$$

The two summations describe the superposition of the signals resulting from the $K=2M+1$ channels and the signal generation due to the N discrete object functions forming the whole object with its finite extension in the x-direction. The phase term now also depends on the transverse location of each light source, $m\cdot x_s$ with $-M\leqslant m\leqslant +M$. For $M=0$, Eq. (4) applies to the conventional schlieren system and reduces to Eq. (3) if the second summation, in the limit, is replaced by an integral.

A particular plane z_i of the object is imaged onto the plane of observation z_6, and the aim of the multi-channel system is that the signal u_6 is caused merely by the respective object function $t_{2,i}(x, z_i)$, while the contributions from all the other object functions are reduced to noise. The number of channels, K, has an influence on the signal-to-noise ratio (SNR), i.e., it is expected that this ratio increases with K (or M). The suppression of noise results from the optical multi-path system that causes a higher weighting of the object plane onto which the plane of observation is focused; or the higher the value of K, the lower the influence of the out-of-focus "slices" on the final signal.

3. Numerical simulation results and discussion

Eq. (4) is evaluated numerically for an optical set-up sketched in Fig. 3. Details of the numerical procedure are given in [3]. The number of light sources or channels, $K = 2M + 1$, and the number of discretisised object "slices" are varied. Only three channels are depicted in Fig. 3. Like shown in this figure, the object plane $z_i = z_0$ is imaged onto the plane of observation z_6. The assumed dimensions in the z-direction and focal lengths of the lenses are also indicated in Fig. 3. The spacing of the multiple sources is chosen here as $x_s = 0.2$ mm, in accordance with values reported in the literature. This value must be adapted to the spatial extention of the object and the influence of this value on the signal quality is not investigated further.

The phase object used in the simulation is presented in Fig. 4. It is equivalent to the laminar jet of a foreign gas exhausted into the ambient constant atmosphere, with the jet axis in the y-direction. The axisymmetric object is assumed to have an extension of ± 25 mm in the x- and z-direction; for the discretisation in the z-direction it is split into 25 planes, equally spaced by 0.5 mm (this parameter whose choice might depend on the properties of the imaging lens was not varied here). The

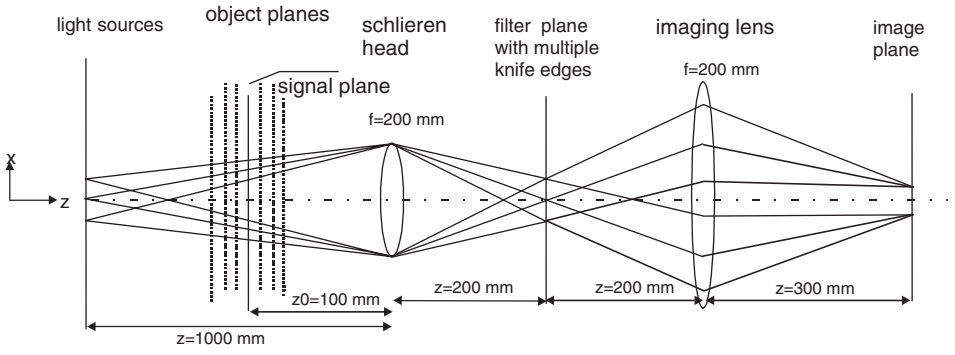

Fig. 3. Multi-channel system with three light sources and geometrical dimensions used in the numerical simultation.

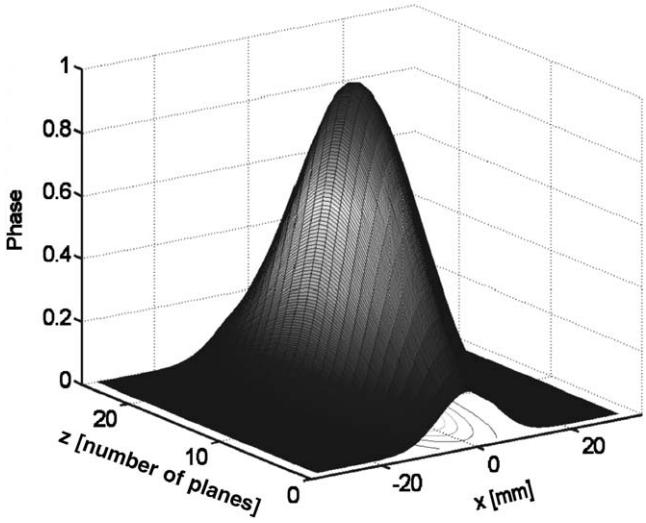

Fig. 4. Optical phase object used in the numerical simulation.

central plane at z_0, imaged onto the plane of observation, is Plane no. 13. The main goal of the simulation is to investigate how well the signal pattern generated by the multi-channel system in the image plane represents the phase distribution in the central plane.

As a first step, that also serves for validating the simulation procedure, we use only a 2D portion of the object shown in Fig 4, namely a slice of width $\Delta z = 2\,\text{mm}$ with a phase distribution as given for the central position, $z_0 = 0$, of the phase object. This slice is a two-dimensional object, not depending on the z-coordinate, and the sharp-focusing schlieren system should not be of any advantage in resolving the object, in comparison to the conventional schlieren system, here characterised by $K = 1$. The schlieren pattern for such a system is known to exhibit two intensity extrema, a minimum on one side and a maximum on the other side of the axis of the assumed (two-dimensional) jet; see, e.g., Fig. 3.11 in Settles [1]. These extrema represent the locations of the change in curvature in the phase distribution. The result of the simulation verifies such a signal pattern (Fig. 5). The signal intensity (in arbitrary units), calculated according to Eq. (4) for different values of $K = 2M + 1$ (up to $K = 15$), is shown as function of the transverse coordinate x. The positions of the extrema are the same for all values of K. The highest contrast in the signal pattern, expressed by the difference between maximum and minimum intensity, is obtained with the conventional schlieren system, i.e., a system with only one channel ($K = 1$). As it had been reported already by Kantrowitz and Trimpi [2], the contrast is lower for the sharp-focusing schlieren systems, the cost that has to be paid for the gain of spatial resolution; the highest contrast is found here for $K = 5$. No direct reason can be given for this value. It can only be said that the lower maximum signal intensity, obviously obtained with the sharp-focusing system, is a consequence of blocking off

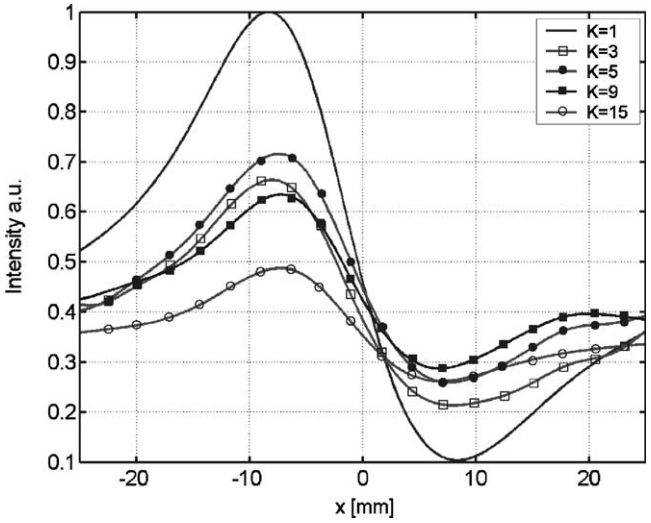

Fig. 5. Signal intensity received in the plane of observation of the various multi-channel systems (number of channels K) for the assumed 2D test object.

part of the light with the "source grid", the system of light sources used in the optical set-up (see Weinstein [3]).

In the simulations with the three-dimensional object of Fig. 4, the result for the signal intensity u_6 obtained for the conventional schlieren system ($K = 1$) is different from the intensity curves calculated for the sharp-focusing systems ($K > 1$), see Fig. 6. The intensity extrema in the signal pattern of the conventional system that were found at positions of approximately $x = \pm 8$ mm in Fig. 5, are now located approximately at $x = \pm 12$ mm. This difference in the patterns obtained for the 2D and the 3D object is a result of the integration of the information along the light path, when a conventional (single channel) schlieren system is used. In contrast to this finding, the positions of the intensity extrema determined for the multi-channel systems all are nearly $x = \pm 8$ mm, as in Fig. 5 for the 2D object. Since the central object plane that is imaged onto the plane of observation in the multi-channel system, has the same phase distribution as the 2D object used in the previous test, the results shown in Fig. 6 demonstrate the possible spatial resolution that can be obtained with the multi-channel schlieren system. As already seen in Fig. 5, the highest signal contrast is achieved with the conventional schlieren system.

For the case investigated here, a spatial resolution of the 3D object is obtained already with the three- and the five-channel system ($K = 3$ and 5, resp.). The further increase of the number of channels does not result in a noticeable improvement of the spatial resolution. This is in agreement with respective findings of Collicott and Salyer [4] who did not increase the number of channels beyond 5. The existence of an optimum for the number of channels can be explained qualitatively with the properties of the imaging lens: With increasing number of channels one increases the

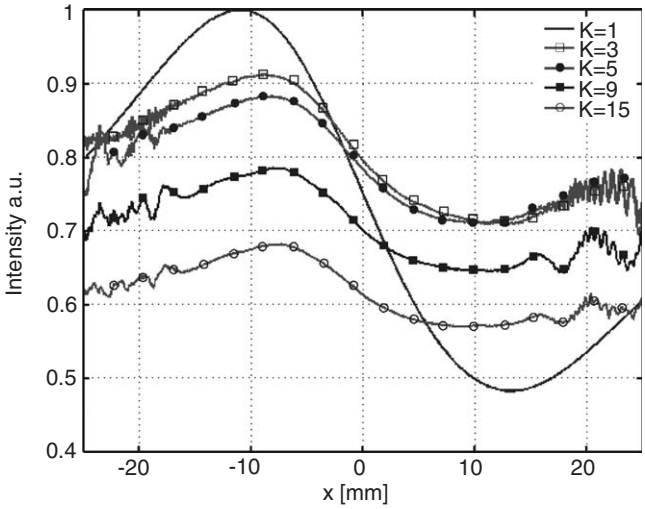

Fig. 6. Signal intensity received in the plane of observation of the various multi-channel systems (number of channels K) for the 3D object shown in Fig. 4. The scattering of the data curves at the outer edge is a numerical effect, resulting from a decrease of the number of channels that overlap in these regions of the object.

aperture angle of the lens and the f-number decreases, thus improving the focusing quality, but only until the maximum aperture is reached.

The dependence of the focusing quality on the number of channels K can be evidenced by defining a signal-to-noise ratio SNR:

$$\mathrm{SNR} = \frac{P_{\mathrm{Signal}}}{P_{\mathrm{Noise}}}. \tag{5}$$

P_{Signall} is the power in the signal contributed by the object plane that is focused onto the plane of observation, in our case the central plane at z_0, and P_{Noisee} is the power contributed to the signal by all object planes that are out of focus. Such SNR values are determined for three different objects: the thin 2D object with $\Delta z = 2\,\mathrm{mm}$ for which results are presented in Fig. 5, the whole 3D object shown in Fig. 3 that has an extension of $\Delta z = \pm 12\,\mathrm{mm}$, and a portion cut from the 3D object covering the central part along a distance of $\Delta z = \pm 6\,\mathrm{mm}$. Values $\mathrm{SNR} > 1$ indicate a spatial resolution of the phase distribution investigated, i.e., the signal from the plane onto which the plane of observation is focused is higher than the noise from the out-of-focus sections of the 3D object, see Fig. 7. The data for the conventional schlieren system ($K = 1$) verify that a spatial resolution is impossible with this system, due to the integration effect. All multi-channel systems investigated show the desired property of spatial resolution of the signals. An optimum is indeed visible in the range of K numbers between 3 and 5, like it had appeared in the previous test.

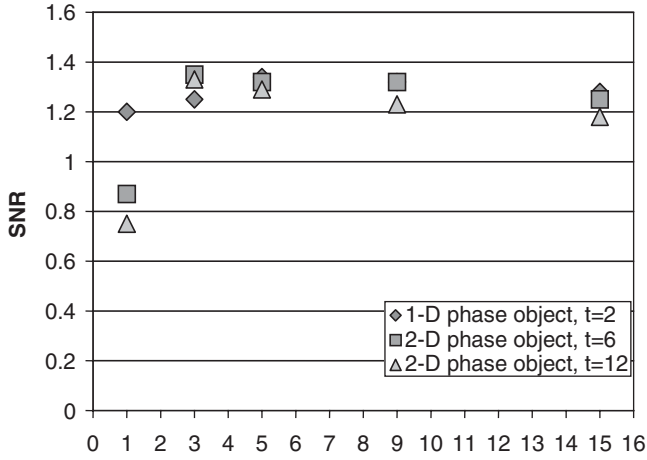

Fig. 7. SNR as function of the number of channels K.

4. Concluding remarks

We have described a way for investigating the properties and potentials of a sharp-focusing schlieren system by means of Fourier analysis. This multi-channel system can be characterised as the superposition of a number of conventional (single-channel) schlieren systems, analoguous to the analysis of Collicott and Salyer [4]. Numerical simulations using a specific test object clearly demonstrate the ability of the system in resolving the three-dimensional phase distribution of this object. The spatial resolution of the information on the properties of the object is a consequence of the multi-channel system. The present results indicate that the optimum of the spatial resolution is reached with a system using five channels or light sources, which is in agreement with observations reported in the literature. Further increase of the number of channels does not increase the quality of this spatial resolution. This result is, to some extent, restricted to the object used in our case study. The agreement with the findings of Collicott and Salyer [4] who performed their studies with a different object may lead to the conclusion, that the optimum of K being in the range of 5 has some general significance.

In the multi-channel system the signal is generated by the superposition of the information carried by a number of light beams or waves that pass through the object in different angular direction. This situation resembles the case of optical tomography where the information on a 3D object is collected from a system of light waves, also transmitted through the object in various directions. We recognise two principal differences of the two methods. One is the way of reconstruction of the 3D object from the data collected by the multi-directional beams: With optical tomography the reconstruction, based on particular mathematical algorithms, is done in the Fourier space, while the reconstruction with the multi-channel system is done in the physical space, i.e., the different signals are superimposed in the image

plane and the object can be scanned physically and step by step with the imaging lens. The second difference is the possible spatial resolution of the object. From the principles of tomography it is known that, for resolving an arbitrary 3D object, it is necessary to pass through the object waves or beams that span a total angular regime of 180°. In the multi-channel system the maximum of this angular regime is controlled by the given aperture of the imaging lens, and it is therefore much smaller than 180°. From this comparison one can conclude that the spatial resolution of a 3D transparent object achievable with optical tomography is higher than that given for a multi-channel or "sharp-focusing" system.

Acknowledgements

This research was supported by Deutsche Forschungsgemeinschaft, Graduiertenkolleg 358 "Optische Messmethoden in den Ingenieurwissenschaften". The authors gratefully acknowledge helpful discussions with Professor J. Böhme at Universität Bochum.

References

[1] Settles GS. Schlieren and shadowgraph techniques. Berlin: Springer; 2001.
[2] Kantrowitz A, Trimpi RL. A sharp-focusing schlieren system. J Aeron Sci 1950;17:311–4.
[3] Weinstein LM. Large-field high-brightness focusing schlieren system. AIAA J 1993;31:1250–5.
[4] Collicott SH, Salyer TR. Noise reduction properties of a multiple-source schlieren system. AIAA J 1994;32:1683–8.
[5] Hanenkamp A. Fourier-optische Beschreibung von Methoden zur Visualisierung von Strömungen mit Dichtunterschieden und Analyse des Sharp-Focusing-Effektes. dissertation, Universität Essen; also published by Aachen: Shaker-Verlag; ISBN: 3-8322-0548-9, 2002.
[6] Taghavi R, Raman G. Visualization of supersonic screeching jets using a phase conditioned focusing schlieren system. Exp Fluids 1996;20:472–5.
[7] Garg S, Settles GS. Measurements of a supersonic turbulent boundary layer by focusing schlieren deflectometry. Exp Fluids 1998;25:254–64.
[8] Wolter H. Schlieren, Phasenkontrast und Lichtschnittverfahren. In: Flügge S, editor. Handbuch der Physik, Vol. 24. Berlin: Springer; 1956. p. 555–645.
[9] Lopez CA. Numerical simulation of a schlieren system from the Fourier optics perspective. AIAA Paper 94-2618; 1994.
[10] Gaskill JD. Linear systems, Fourier transforms, and optics. New York: Wiley; 1978.